

Quarks Production in the Quark-Gluon Plasma Created in Relativistic Heavy Ion Collisions

M. Ruggieri^{a,*}, S. Plumari^{a,b}, F. Scardina^{a,b}, V. Greco^{a,b}

^a*Department of Physics and Astronomy, University of Catania, Via S. Sofia 64, I-95125 Catania*
^b*INFN-Laboratori Nazionali del Sud, Via S. Sofia 62, I-95123 Catania, Italy*

Abstract

In this article we report on our results about quark production and chemical equilibration of quark-gluon plasma. Our initial condition corresponds to a classic Yang-Mills spectrum, in which only gluon degrees of freedom are considered; the initial condition is then evolved to a quark-gluon plasma by means of relativistic transport theory with inelastic processes which permit the conversion of gluons to $q\bar{q}$ pairs. We then compare our results to the ones obtained with a standard Glauber model initialization. We find that regardless of the initial condition the final stage of the system contains an abundant percentage of $q\bar{q}$ pairs; moreover spanning the possible coupling from weak to strong we find that unless the coupling is unrealistically small, both production rate and final percentage of fermions is quite large.

Keywords: Quark-gluon plasma, Relativistic transport theory.

PACS: 12.38.Mh, 25.75.Nq

1. Introduction

In the last decade it has been reached a general consensus that Ultra-relativistic heavy-ion collisions (uRHICs) at the Relativistic Heavy-Ion Collider (RHIC) and the Large Hadron Collider (LHC) create a hot and dense strongly interacting quark and gluon plasma (QGP) [1, 2, 3, 4]. A main discovery has been that the QGP has a very small shear viscosity to density entropy, η/s , which is more than one order of magnitude smaller than the one of water [5, 6], and close to the lower bound of $1/4\pi$ conjectured for systems at infinite strong coupling [7]. According to the standard picture of ultrarelativistic heavy ion collisions, before the collision the two colliding nuclei can be represented as two thin sheets of color-glass condensate [8, 9, 10] which produce, immediately after the collision, a configuration of strong longitudinal chromoelectric and chromomagnetic fields named the glasma, see [11, 12, 13] for reviews.

An interesting problem of uRHICs is the dynamical evolution of the high energy system made mainly of gluons, obtained from the decay of the glasma flux tubes, to a locally thermalized and eventually chemically equilibrated quark-gluon plasma. This problem has been discussed

^{*}Corresponding author.

Email address: marco.ruggieri@lns.infn.it (M. Ruggieri)

previously in [27] where quark-antiquark production rate is computed by means of the solution of the Dirac equation in the background of the strong initial plasma field, and in [21] by simulations based on relativistic transport theory (RTT) which is a fruitful theoretical tool to study the evolution of QGP produced in heavy ion collisions [14, 15, 16, 17, 18, 19, 20, 21, 22, 23]. In this article we follow closely Ref. [21] and in some sense the present study is a continuation of [21]: in fact in [21] several aspects have not been investigated, in particular the role of the initial non-equilibrium distribution on $q\bar{q}$ production times and on the chemical equilibration of the QGP, as well as a study of the coupling dependence of the aforementioned quantities. These are the aspects we study in the present article.

We are interested to compute the $q\bar{q}$ production rate initializing simulations by a pure gluon plasma with the spectrum computed within the classical Yang-Mills (CYM) theory of the plasma. The evolution of the initial condition is then achieved by relativistic transport theory. The simulations with the CYM spectrum are started at $\tau_0 = 0.2$ fm/c, hence assuming in this time range the initial longitudinal gluon fields have decayed (the decay time is of the order of $1/Q_s$ with Q_s corresponding to the saturation scale) and to populate the transverse momentum space (in the initial plasma the fields are purely longitudinal hence the p_T -spectrum at $\tau = 0^+$ is zero). Within our approach we cannot discuss if and how quarks are produced before $\tau = \tau_0$; however we find that even neglecting the possible quark formation for $\tau < \tau_0$ the QCD inelastic processes are efficient enough to obtain a final state which consists mainly of $q\bar{q}$ pairs rather than gluons.

We also consider the problem of the chemical equilibration of the QGP once quarks are formed. For a system of quarks and gluons thermalized at the same temperature T the equilibrium value for $R \equiv (N_q + N_{\bar{q}})/N_g$ is given by

$$R_{eq} = \frac{9 m_q^2(T) K_2(m_q/T)}{4 m_g^2(T) K_2(m_g/T)} ; \quad (1)$$

for example if quarks and gluons are massless one finds easily $R_{eq} = 9/4$ at chemical equilibrium. We find that changing the initial distribution from a Glauber model to a CYM spectrum has some effect on the chemical equilibration, the effect being more relevant in the case of weak coupling.

In the present study we use the quasiparticles to identify quarks and gluons propagating in the QGP. In particular we consider the case of massless quasiparticles, which corresponds to a fluid with the perfect massless gas equation of state; the case of massive quasiparticles with temperature independent masses, corresponding to a fluid with the equation of state of an ideal massive gas. Finally we also consider the case of energy density dependent quasiparticle masses, with masses fixed by requiring the equation of state of the fluid is the one of QCD as it is measured on the lattice [26].

The plan of the article is as follows. In Section II we review relativistic transport theory which is the base of our simulation code. In Section III we summarize our results concerning formation time of quarks as well as chemical equilibration of the QGP, when we initialize simulations starting either from a Glauber model or a CYM spectrum; in this Section we consider the cases of massless as well as massive quasiparticles, in the latter case considering both constant and temperature dependent masses. Finally in Section IV we draw our conclusions.

2. Relativistic Transport Theory

In our study we simulate the evolution of the QGP fireball by means of a code based on the solution of the relativistic kinetic Boltzmann-Vlasov equation for the gluon and quark distribution function,

$$[p^\mu \partial_\mu + M(x) \partial_\mu M(x) \nabla^\mu] f(x, p) = C[f], \quad (2)$$

where $\nabla^\mu = \partial_p^\mu$ denotes the gradient with respect to momenta and $M(x)$ corresponds to the quasi-particle mass: we have made the dependence of this mass on the space-time coordinates explicit, which comes from the fact that in quasiparticle models M is a function of energy density [26] and the latter changes in space and time due to the expansion as well as to the interactions. It is useful to remind at this point that the use of a quasiparticle mass in the above equation implies that the QGP fluid has a given equation of state: if we take $M = 0$ it means we simulate a fluid with a perfect gas equation of state $\varepsilon = 3P$; on the other hand if M is fixed with a temperature dependence according to [26] then it is equivalent to state that the QGP fluid evolves with the lattice QCD equation of state once the local kinetic equilibrium is reached.

In Eq. (2) the collision integral takes the form

$$C[f] = \int_2 \int_{2'} \int_{1'} (f_1 f_2' - f f_2) |\mathcal{M}|^2 \delta^4(p + p_2 - p_1' - p_2') d\Gamma_2 d\Gamma_1' d\Gamma_2', \quad (3)$$

where \mathcal{M} denotes the invariant amplitude for the process $12 \rightarrow 1'2'$ and $2E_i d\Gamma_i = d^3 p_i / (2\pi)^3$. Both elastic as well as inelastic processes contribute to the invariant amplitude. In this work we follow [21] and we consider only the two body processes. In particular all the elastic cross sections we take have the form

$$\frac{d\sigma_{\text{elastic}}}{dt} \propto \frac{\alpha_s}{(t - m_D^2)^2}, \quad (4)$$

where t denotes the invariant Mandelstam variable and $m_D = 0.7$ GeV is used as an infrared regulator and determines how isotropic the cross section is (the smaller m_D the more forward peaked the cross section). The overall factor in the previous equation changes channel by channel ($q\bar{q}$, qq , qg , $\bar{q}g$ and gg) as in [21].

In this study we fix the value of α_s and compute the relevant cross sections. In order to estimate an appropriate value of α_s we use the total cross section for gg scattering among massless gluons and require that the value of η/s obtained by this massless gluon-gluon scattering is approximately the one used in hydrodynamics and/or transport simulations. To estimate such a coupling we use the approximate kinetic theory relation [22, 23]

$$\sigma_{gg}^{\text{massless}} = \frac{3}{10} \frac{T}{n} \frac{1}{\eta/s}, \quad (5)$$

which, for a reference temperature of $T = 0.3$ GeV gives $\alpha_s = 0.7$ for $\eta/s = 2/4\pi$ as used in heavy ion collisions simulations [14, 20, 34]. A value of $\alpha_s \approx 0.9$ would be required for $\eta/s = 1/4\pi$, which certainly would cause the gluons-to-quarks processes to be even faster but which does not

affect considerably the final quark spectra as well as the final gluon number to quark number ratio, see next Section. We will also consider the case of a running strong coupling,

$$\alpha_s(T) = \frac{2\pi}{9} \frac{1}{\log(\pi T/\Lambda)} , \quad (6)$$

with $\Lambda = 0.2$ GeV; for example at $T = 0.3$ GeV one finds $\alpha_s \approx 0.4$.

For the inelastic processes between quarks and gluons $gg \leftrightarrow q\bar{q}$ we have $\mathcal{M} = \mathcal{M}_s + \mathcal{M}_t + \mathcal{M}_u$. For the massless case the cross sections for such processes are the textbook pQCD cross section for jet production in high-energy proton-proton collisions. With massive quarks the calculations are the Combridge cross sections [24, 25] used to evaluate heavy-quark production. In our case we have considered a finite mass for both gluons and quarks together with a dressed gluon propagator. It is worth to mention here that the cross section for the process at hand is dominated by the t - and u -channel and their interference, while the s -channel alone is negligible. The squared matrix element of the t -channel is given by

$$|(t - m_q^2)\mathcal{M}_t|^2 = \frac{8}{3}\pi^2\alpha_s^2 \left[(m_q^2 - t)(m_q^2 - u) - 2m_q^2(t + m_q^2) - 4m_q^2m_g^2 - m_g^4 \right] , \quad (7)$$

where m_q , m_g denote the quasiparticle masses for quarks and gluons respectively.

3. Results

3.1. The massless case

In the present work we focus on two different initial conditions for our simulations. The first one is named thermal Glauber (Th-Glauber) in which we distribute particles in transverse coordinate space according to the usual Glauber model with the standard mixture $0.85N_{part} + 0.15N_{coll}$, while distributing particles in boost invariant way along the longitudinal direction; initial momentum space distribution corresponds to a thermal distribution in transverse momentum space and a boost invariant distribution in the longitudinal direction with $y = \eta$, with y and η denoting momentum and space-time rapidities respectively. The other initial condition we use in our simulations is named CYM initialization, in which transverse plane particle distribution corresponds to a Glauber model with N_{coll} scaling [34] while initial p_T -distribution is obtained by the solution of classical Yang-Mills equations [35]; also in this case we assume longitudinal boost invariance and $y = \eta$.

In Fig. 1 we plot the time evolution of the particle number for the several initializations we consider in this work. On the horizontal axis we measure the time difference $\tau - \tau_0$ where τ_0 corresponds to the initialization time; in this study we chose $\tau_0 = 0.6$ fm/c for the case of the Glauber initialization and $\tau_0 = 0.2$ fm/c for the CYM initialization. In the latter case we assume a smaller initialization time because we do not need to assume any pre-thermalization, which instead is assumed in the Glauber initialization. In the figure, N_{quarks} corresponds to the total number of quarks *plus* the total number of antiquarks. The results we present in this article correspond to simulations run for Au-Au collisions at RHIC energy, for $b = 2.5$ fm; the initial gluon multiplicity is $dN_g/dy = 1040$.

In Fig. 2 we plot the results for initial and final particle spectra at midrapidity $|y| \leq 0.5$. In the figure we do not show initial spectra for quarks because we assume that at $\tau = \tau_0$ there are no

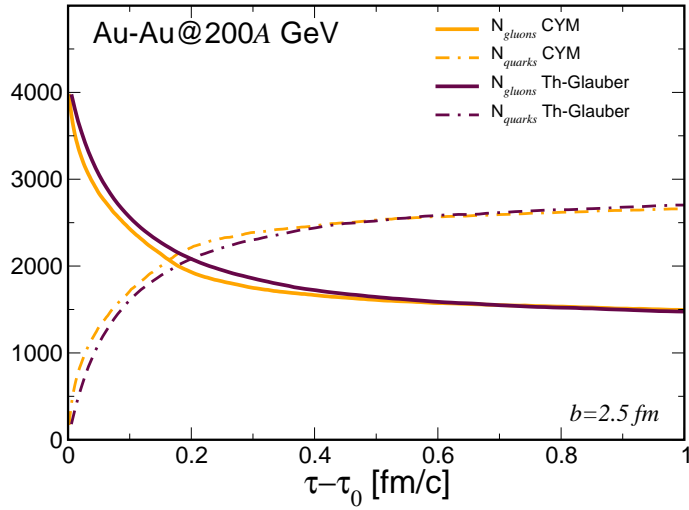


Figure 1: Early time evolution of particle number for thermal Glauber (indigo) and CYM (orange) initializations. Initial gluon number corresponds to $dN_g/dy = 1040$.

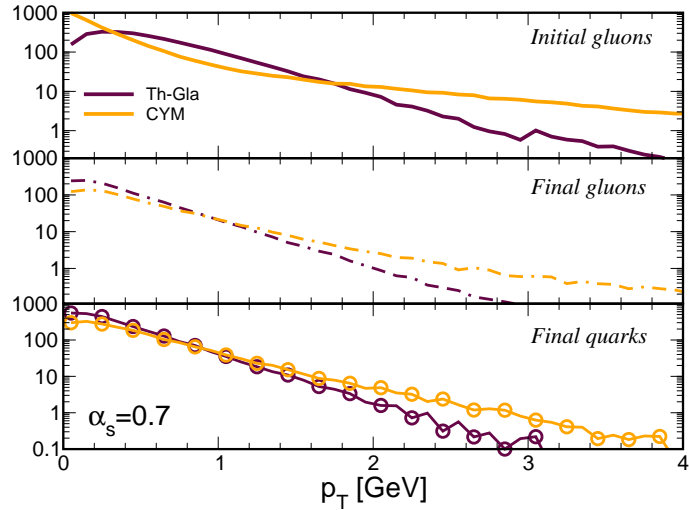


Figure 2: Time evolution of particle spectra for thermal Glauber (indigo) and CYM (orange) initializations. In both simulations the initial gluon number corresponds to $dN_g/dy = 1040$.

quarks in the system. This might be a crude approximation for the Glauber initialization since it is equivalent to assume that some dynamics took place up to $\tau = \tau_0$ to thermalize the system in the transverse plane, nevertheless affecting only gluons and not producing any quark; nevertheless for the early times initializations this might be not a so bad approximation since we are only assuming that within a time of the order of $1/Q_s \approx \tau_0$ the system is mainly made of gluons, then as soon as we initialize the dynamics the QCD processes cause the conversion of gluons to quarks. We remark that a more realistic condition including a finite number of quarks can only make stronger

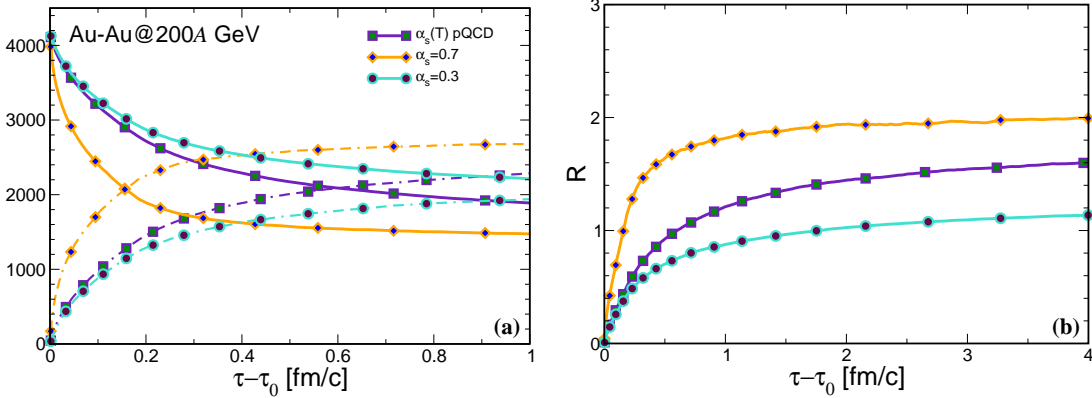


Figure 3: *Left panel*: Early time evolution of gluons and fermions number for the case of CYM initialization and several choices for the coupling. *Right panel*: ratio of total quark number over gluon number as a function of time. Data style convention in the right panel is the same as the one in the left panel. Calculations correspond to Au-Au collision at $\sqrt{s} = 200A$ GeV and $b = 2.5$ fm.

our final result that quark production is quite fast and abundant.

The results summarized in Figg. 1 and 2 are obtained assuming a value of $\alpha_s = 0.7$. As a reference we remind that this value of the coupling corresponds to a value of $\eta/s \approx 2/4\pi$ at temperature $T = 0.3$ GeV, which is not far from the value of η/s which is normally used in ultrarelativistic heavy ion collisions simulations to quantify the dissipation of the QGP fluid.

In the left panel of Fig. 3 we plot the gluon and total quark numbers as a function of time, focusing on the CYM initialization and on the early stage of the time evolution of the fireball. For other initializations we obtain similar results which are not shown for space sake. In the figure we have shown three different cases corresponding to three different choices for α_s . In particular, diamonds and circles correspond to a fixed value of α_s , namely $\alpha_s = 0.7$ and $\alpha_s = 0.3$ respectively; on the other hand squares correspond to the case of the temperature dependent α_s given by Eq. (6).

The definition of a quark formation time τ_q is quite arbitrary, therefore we define it as the time necessary to have a mixture made of 50% of quarks plus antiquarks and 50% of gluons, corresponding to $R = 1$ with $R = (N_q + N_{\bar{q}})/N_g$. As already discussed in the case $\alpha_s = 0.7$ the system is very efficient in converting gluons to quarks, in fact the total number of quarks becomes comparable to the one of gluons within $\tau_q \approx 0.15$ fm/c. It is interesting that in the case of the perturbative running coupling, indigo data in Fig. 3, even if the average coupling is smaller than the case $\alpha_s = 0.7$ (of about a factor of 1.5 when averaged on the fireball) the system is still quite efficient in producing quarks via the QCD inelastic processes. In fact in this case we find $\tau_q \approx 0.6$ fm/c, which is about a factor of 4 larger than the time required in the case $\alpha_s = 0.7$ but still very fast compared to the time evolution of the fireball. Finally in the case $\alpha_s = 0.3$ we find that quark production is quite slow compared to the previous cases, having $\tau_q \approx 2$ fm/c which is approximately 3.3 times larger than τ_q obtained within the perturbative running coupling and approximately 1/2 of the lifetime of the QGP in the fireball.

In the right panel of Fig. 3 we plot the ratio $R = (N_q + N_{\bar{q}})/N_g$ again for the case of the CYM initialization, for the same values of α_s considered in the left panel of the same figure. In

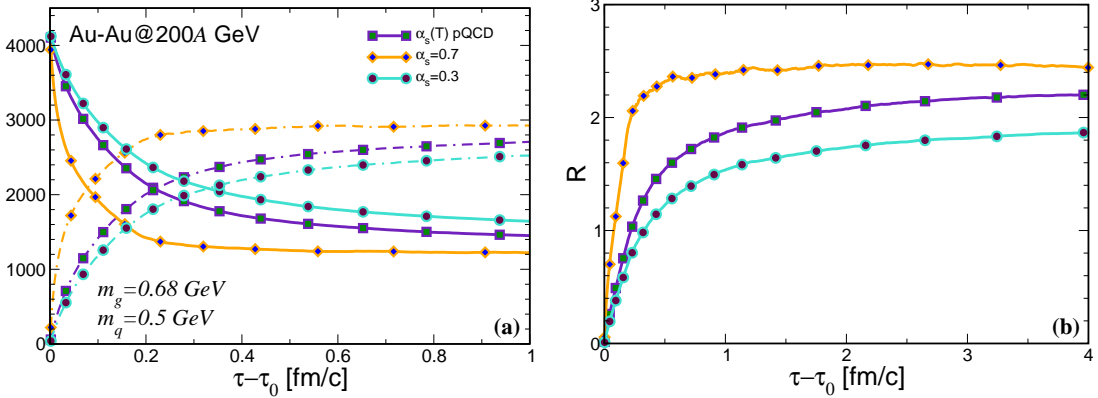


Figure 4: *Left panel*: Early time evolution of gluons and fermions number for the case of CYM initialization and several choices for the coupling, for the case of massive quasiparticles. *Right panel*: ratio of total quark number over gluon number as a function of time. Data style convention in the right panel is the same as the one in the left panel. Calculations correspond to Au-Au collision at $\sqrt{s} = 200A$ GeV and $b = 2.5$ fm.

the case of $\alpha_s = 0.7$ the system reaches the equilibrium value for a massles gas, $R = 2$, in a quite short time. On the other hand in the case of a running perturbative coupling, even if the quark production has been efficient in the early stages after the collision, the system is not able to chemically equilibrate onto the chemical equilibrium value within the lifetime of the QGP in the fireball; in fact R saturates to a somewhat smaller value ≈ 1.7 while $R = 9/4$ at equilibrium. Finally in the case of weak coupling $\alpha_s = 0.3$ we find the value $R \approx 1.2$ is reached within the lifetime of the fireball, meaning the system is unable to reach chemical equilibration in weak coupling regime even though quark fraction is still abundant.

3.2. The massive case: temperature independent masses

In the left panel of Fig. 4 we plot the gluon and total quark numbers as a function of time, for the case of massive quasiparticles. In order to emphasize the role of a finite mass for the quasiparticles, as well as of the different mass among quarks and gluons, we have restricted ourselves to the case of temperature independent masses. According to the results of [26] we have chosen the ratio of the gluon to quark mass to be $3/2$, neglecting a mild temperature dependence of the masses in the range of temperature relevant for the evolution of the fireball at RHIC energy. We have chosen the quark mass to be $m_q = 0.5$ GeV in agreement with the results of [26]. We find that regardless of the choice for the coupling, considering massive quasiparticles amounts to increase the quarks to gluons number ratio R of about 30% along with a general acceleration of τ_q , compare Figg. 3 and 4. This is easily understood because in this case quarks are lighter than gluons and statistically it is easier to convert a pair of gluons into a $q\bar{q}$ pair.

3.3. The massive case: temperature dependent masses

In the left panel of Fig. 5 we plot the gluon and total quark numbers as a function of time, for the case of massive quasiparticles with a temperature dependent mass. The quasiparticle masses are computed according to [26] in order to fit the lattice thermodynamics data; in other words, the

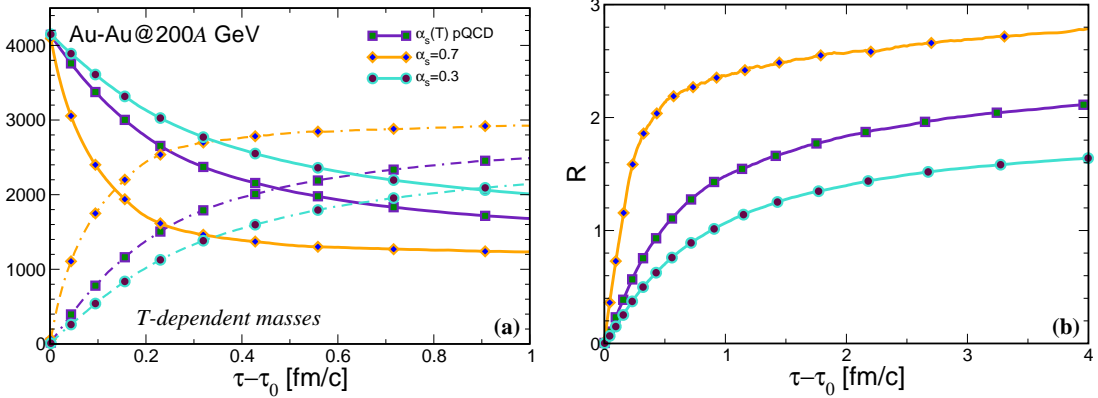


Figure 5: *Left panel*: Early time evolution of gluons and fermions number for the case of CYM initialization and several choices for the coupling, for the case of T -dependent masses. *Right panel*: ratio of total quark number over gluon number as a function of time. Data style convention in the right panel is the same as the one in the left panel. Calculations correspond to Au-Au collision at $\sqrt{s} = 200A$ GeV and $b = 2.5$ fm.

masses we consider in this section are such that the equation of state of the fluid we simulate is that of lattice QCD. Left panel of Fig. 5 focuses on the very early history of the fireball; we find that this case does not differ in a relevant way from the case of temperature independent masses discussed in the previous subsection. In fact also in this case perturbative QCD processes lead to fast quarks production. However a considerable quantitative difference is found for the final values of the ratio R of quarks to gluons, which is more evident in the case of strong coupling $\alpha_s = 0.7$. Indeed in the case of temperature independent masses of Fig. 4 we found that R approaches ≈ 2.4 within few fm/c; instead in the case of temperature dependent masses we find that $R \approx 3$ at the end of the evolution.

On the other hand, for the running coupling constant case, circles in Fig. 5, we find that the use of the temperature dependent masses does not affect very much the result obtained within fixed masses. This can be understood *a posteriori* since the quark and gluon masses in Fig. 4 do not differ too much from those of Fig. 5, besides the peripheral cells where the temperature is smaller thus the masses are larger, but the coupling is smaller than the case $\alpha_s = 0.7$ (roughly corresponding to $\eta/s = 0.15$) implying the system is less effective in converting gluons to quarks. The regions of the fireball where temperature is close to the critical temperature are still important, because the smaller the temperature the larger the ratio R in this case, but these regions can be effective in the production of quarks only if the coupling is large enough, which is achieved by the case $\alpha_s = 0.7$ but not in the case of the running perturbative coupling. This explains the results on the right panel of Fig. 5.

3.4. CYM versus Glauber initializations

In this subsection we compare the evolution of the quarks to gluons ratio obtained by the Glauber and the CYM initializations, for both cases of strong fixed and temperature dependent couplings. The cases of both temperature dependent and constant masses are considered. This comparison is instructive since it permits to enlighten about the role of the different initialization

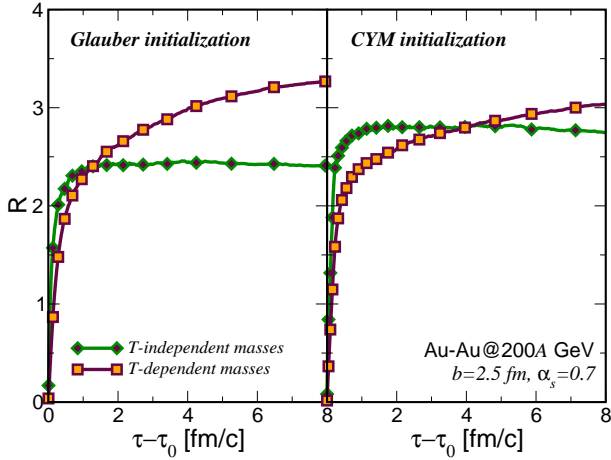


Figure 6: Comparison of the ratio R for the Glauber and the CYM initializations. Left panel corresponds to Glauber initialization, right panel to CYM initialization. Calculations are performed with a fixed $\alpha_s = 0.7$, for Au-Au collision at $\sqrt{s} = 200A$ GeV and $b = 2.5$ fm.

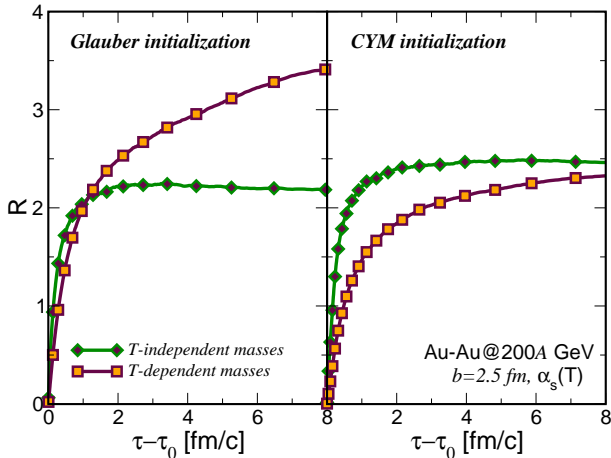


Figure 7: Comparison of the ratio R for the Glauber and the CYM initializations. Left panel corresponds to Glauber initialization, right panel to CYM initialization. Calculations are performed with a temperature dependent α_s , for Au-Au collision at $\sqrt{s} = 200A$ GeV and $b = 2.5$ fm.

on quark production. It is useful to remind here that the case of temperature dependent masses corresponds to assume the QGP fluid is characterized by the equation of state of lattice QCD.

In Fig. 6 we plot the evolution of R as a function of time for the Glauber initialization (left panel) and the CYM initialization (right panel). The results are shown for the cases of constant mass and temperature dependent mass, with perturbative running and fixed strong coupling (the latter corresponding to $\alpha_s = 0.7$). In the case of strong coupling, left panel of Fig. 6, we find that for the Glauber initialization switching from a constant mass to a thermal one leads to an increase of the ratio R at later times. This is mainly due to the fact that the number of gluons decreases

(and that of quarks increases) continuously in the case of a temperature dependent mass, while it saturates after a time of about 2 fm/c in the case of a constant mass. We find the same result for the CYM initialization, even if in this case the effect of turning on a temperature dependent mass is milder. However, the conclusion is that regardless the initial condition chosen in the simulation, at later times the fireball consists of about 80% of quarks and only 20% of gluons even starting from a condition in which the system is made of gluons only. Finally in Fig. 7 we plot the ratio R for the case of $\alpha_s(T)$.

4. Conclusions

In this Article we have studied quark production from a pure gluon plasma produced in ultrarelativistic heavy ion collisions. Our main goal has been to study how a pure gluon plasma evolves dynamically to a quark-gluon plasma by means of QCD inelastic processes; the impact of the initial condition on the relative composition in quarks and gluons and on quark production times has been investigated. We have considered two different kinds of initializations: the usual Glauber initialization and one based on the gluon spectrum obtained by the classical Yang-Mills theory (CYM) of the glasma. Given the initial condition, we have evolved it according to relativistic transport theory, and quark production has been taken into account by means of QCD inelastic processes.

The definition of a quark formation time τ_q is quite arbitrary, therefore we have defined it as the time necessary to have a mixture made of 50% of quarks plus antiquarks and 50% of gluons. We have found that the initial condition does not have a relevant impact on τ_q ; this is true both if we consider a pure perturbative coupling and a strong coupling regime in which α_s is chosen scale-independent and of magnitude such that the corresponding η/s is in the range $1 \div 2$. The coupling has some effect on τ_q : changing the coupling from strong to weak we have obtained τ_q increases about of a factor 4; nevertheless even in weak coupling we find abundant fermion production takes place within $\tau \leq 1$ fm/c.

We have then computed the ratio $R \equiv (N_q + N_{\bar{q}})/N_g$ and we have found it is affected not only by the coupling strength but also on the kind of quasiparticle mass we implement in the simulation. In the case of strong coupling we have found that regardless of the initial condition the ratio R approaches about $2.5 \div 3.5$; in the case of weak coupling the effect of the initialization is quite strong for the case of temperature dependent masses, being instead not so strong in the case of massive quasiparticles with a constant mass. It is interesting that even in the weak coupling case the asymptotic $R \approx 2 \div 2.5$ signaling an abundant production of quarks plus antiquarks has been achieved during the fireball's lifetime.

Among the many interesting aspects which deserve further study we briefly mention here the possibility to include, in future studies, the Bose-Einstein enhancing factors in the collision integral which might lead to a transient condensate in the very early stages of the glasma evolution [28, 29, 30, 31, 32], hence affect the conversion of gluon to quarks [36]. Moreover it will be interesting to compare the quark production in QGP studied in the present article with the one obtained by the shattering of the flux tubes via the Schwinger mechanism, following the lines of [33]. Both these problems will be the subject of forthcoming publications.

Acknowledgements. We acknowledge B. Schenke and R. Venugopalan for kindly providing us the data of the initial CYM spectra and for fruitful correspondence. We also acknowledge A. Puglisi for enlightening discussions. V. G., M. R. and F. S. acknowledges the ERC-STG funding under the QGPDyn grant.

- [1] STAR, J. Adams et al., Nucl. Phys. **A757**, 102 (2005); PHENIX, K. Adcox et al., Nucl. Phys. **A757**, 184 (2005).
- [2] K. Aamodt et al. [ALICE Collaboration], Phys. Rev. Lett. **105**, 252302 (2010).
- [3] B. V. Jacak and B. Muller, *Science* **337**, 310 (2012).
- [4] R. J. Fries, V. Greco and P. Sorensen, Ann. Rev. Nucl. Part. Sci. **58** (2008) 177
- [5] L. P. Csernai, J. I. Kapusta and L. D. McLerran, Phys. Rev. Lett. **97** (2006) 152303
- [6] R. A. Lacey *et al.*, Phys. Rev. Lett. **98**, 092301 (2007).
- [7] P. Kovtun, D. T. Son, and A. O. Starinets, Phys. Rev. Lett. **94**, 111601 (2005).
- [8] L. D. McLerran and R. Venugopalan, Phys. Rev. D **49**, 2233 (1994)
- [9] L. D. McLerran and R. Venugopalan, Phys. Rev. D **49**, 3352 (1994)
- [10] L. D. McLerran and R. Venugopalan, Phys. Rev. D **50**, 2225 (1994).
- [11] F. Gelis, E. Iancu, J. Jalilian-Marian and R. Venugopalan, Ann. Rev. Nucl. Part. Sci. **60**, 463 (2010).
- [12] L. McLerran, arXiv:0812.4989 [hep-ph]; hep-ph/0402137.
- [13] F. Gelis, Int. J. Mod. Phys. A **28**, 1330001 (2013).
- [14] M. Ruggieri, F. Scardina, S. Plumari and V. Greco, Phys. Rev. C **89**, 054914 (2014).
- [15] Z. Xu and C. Greiner, Phys. Rev. C **79** (2009) 014904
- [16] Z. Xu, C. Greiner and H. Stocker, Phys. Rev. Lett. **101** (2008) 082302
- [17] E. L. Bratkovskaya, W. Cassing, V. P. Konchakovski and O. Linnyk, Nucl. Phys. A **856** (2011) 162
- [18] G. Ferini, M. Colonna, M. Di Toro and V. Greco, Phys. Lett. B **670**, 325 (2009)
- [19] S. Plumari and V. Greco, AIP Conf. Proc. **1422** (2012) 56
- [20] M. Ruggieri, F. Scardina, S. Plumari and V. Greco, Phys. Lett. B **727**, 177 (2013).
- [21] F. Scardina, M. Colonna, S. Plumari and V. Greco, Phys. Lett. B **724**, 296 (2013).
- [22] S. Plumari, A. Puglisi, M. Colonna, F. Scardina and V. Greco, J. Phys. Conf. Ser. **420**, 012029 (2013).
- [23] S. Plumari, A. Puglisi, F. Scardina and V. Greco, Phys. Rev. C **86**, 054902 (2012).
- [24] B. L. Combridge, Nucl. Phys. B **151**, 429 (1979).
- [25] T. S. Biro, P. Levai and B. Muller, Phys. Rev. D **42**, 3078 (1990).
- [26] S. Plumari, W. M. Alberico, V. Greco and C. Ratti, Phys. Rev. D **84**, 094004 (2011).
- [27] F. Gelis, K. Kajantie and T. Lappi, Phys. Rev. Lett. **96**, 032304 (2006); T. Lappi, J. Phys. G **32**, S179 (2006).
- [28] J. P. Blaizot, J. Liao and L. McLerran, Nucl. Phys. A **920**, 58 (2013).
- [29] J. P. Blaizot, F. Gelis, J. F. Liao, L. McLerran and R. Venugopalan, Nucl. Phys. A **873**, 68 (2012).
- [30] J. P. Blaizot, F. Gelis, J. Liao, L. McLerran and R. Venugopalan, Nucl. Phys. A **904-905**, 829c (2013).
- [31] J. Liao, Nucl. Phys. A **928**, 247 (2014).
- [32] F. Scardina, D. Perricone, S. Plumari, M. Ruggieri and V. Greco, arXiv:1408.1313 [nucl-th].
- [33] R. Ryblewski and W. Florkowski, Phys. Rev. D **88**, 034028 (2013).
- [34] B. Schenke, P. Tribedy and R. Venugopalan, Phys. Rev. Lett. **108**, 252301 (2012); C. Gale, S. Jeon, B. Schenke, P. Tribedy and R. Venugopalan, Phys. Rev. Lett. **110**, no. 1, 012302 (2013).
- [35] B. Schenke, P. Tribedy and R. Venugopalan, Phys. Rev. C **89**, no. 2, 024901 (2014).
- [36] J. P. Blaizot, B. Wu and L. Yan, Nucl. Phys. A **930**, 139 (2014).